Metallurgical Science and Technology

A journal published by Teksid Aluminum twice a year

Vol. 21 No. 1, June 2003

SILICON PARTICLE DAMAGE IN A THIXOCAST A356 ALUMINIUM ALLOY*

P. Leo, E. Cerri

INFM- Innovation Engineering Department, University of Lecce, Via per Arnesano, 73100, Lecce, Italy

" This paper was presented at the "29° convegno nazionale AIM", Modena 13-14-15 november 2002"

SILICON PARTICLE DAMAGE IN A THIXOCAST A356 ALUMINIUM ALLOY

P. Leo, E. Cerri

INFM- Innovation Engineering Department, University of Lecce, Via per Arnesano, 73100, Lecce, Italy

Abstract

The thixocast A356 aluminium alloy shows high mechanical properties if compared to those of the same alloy obtained by traditional foundry methods. This improvement is due to the fine and homogeneous globular microstructure that is obtained by thixocasting; traditional heat treatments are always possible. In the present study, samples of A356 thixocast aluminium bars have been solution treated and aged. The precipitation hardening has been monitored by hardness and electrical conductivity measurements. Tensile tests have been performed on heat-treated samples and the importance of silicon particles in the fracture process has been put in evidence.

Riassunto

La lega di alluminio A356 thixocolata esibisce proprietà meccaniche notevolmente superiori a quelle della stessa lega ottenuta secondo i tradizionali metodi di fonderia. Questo miglioramento è imputabile alla microstruttura globulare, fine ed omogenea, che è alla base del processo di thixoformatura e sulla quale si può ulteriormente intervenire con i tradizionali trattamenti termici. In questo studio provini derivanti da barre di alluminio A356 thixocolate sono stati solubilizzati ed invecchiati ed il processo di precipitazione è stato seguito mediante misure di conducibilità termica e di durezza. Lo studio della lega trattata termicamente e deformata mediante prove di trazione ha evidenziato il ruolo delle particelle di silicio nel processo di frattura.

INTRODUCTION

Foundry aluminium alloys based on the Al-Si system are widely used in the automotive field since they associate excellent fluidity and castability, good resistance to corrosion and mechanical properties. The mechanical properties and fracture behaviour are influenced by the presence of shrinkage porosity, dross and oxides (2), by dendrite dimensions (1), and also by Si particles shape and dimension present in the eutectic areas (3,4). In fact, fracture and decohesion of silicon particles can decrease mechanical properties to fracture (3). Moreover, Al-Si alloys are characterised by a wide temperature range in the semi-solid region, which makes them particularly suitable to be thixocast. The advantages that the thixocasting process offers to the production cycle (for example net shape products, the reduction of cycle times and mould wear) and the good mechanical properties of the components propose this forming method with excellent use credentials. In particular, thixomolded and heat-treated T6 products have mechanical characteristics superior to those obtained by traditional foundry methods. Among aluminium alloys of the 3xx series, A356 and 357 are the most used for thixocasting .

A356 contains silicon but also magnesium and iron as main alloy elements. It shows an excellent castability together with a good resistance to corrosion and good tensile strength. The disadvantages of this alloy maybe are its low elastic module and precipitation hardening. The interest for thixomolding also comes from the possibility to improve T6 hardness values respect to the traditionally cast alloy.

Aluminium alloys usually present a ductile fracture which occurs at low rate after plastic deformation, with a localised necking. The ductile fracture process usually originates with a nucleation of microvoids and continues with their coalescence to form a macrocrack propagating in a direction perpendicular to the applied strain. In the Al-Si-Mg alloys, as the 356, silicon particles play an important role on the fracture process because of their breaking or decohesion from the matrix. This work studies the microstructure damage occurring, after the application of a plastic deformation, in the thixocast A356 aluminium alloy, solution treated and aged for different temperatures and times. This paper includes a microstructure investigation of the as-thixo and heat-treated samples, electrical conductivity and hardness measurements and the statistical analysis of damage to be correlated with mechanical properties.

“ This paper was presented at the “29° convegno nazionale AIM”, Modena 13-14-15 november 2002"

EXPERIMENTALS

The A356 alloy, whose chemical composition is reported in Table 1, has been supplied by Aluminium Pechiney in the form of cylindrical thixocast bars with a length of 197 mm and 18 mm in diameter.
Cylindrical samples of 10 mm in height have been cut from the bars by a diamond saw for heat treatments. Samples for tensile tests have been obtained by electroerosion with a section of 5.5x5 mm^2.Heat treatment at 540°C for 1, 2, 4, 8, 16 hours has been performed to study the structure evolution at high temperature.The aging has been performed at 160°C and 200°C for 0,5, 1, 2, 8, 16, 25 hours after exposure at 540°C for 1 h.
Samples for tensile tests have been solubilised at 540°C for 1 hour, quenched and aged at 160°C for 1, 4, 25 h. and at 200°C for 0,5 and 4 h.
Rockwell F hardness measurements and tensile tests specimen have been carried out respectively on an Ernst Hardness Tester Type AT130D and on an INSTRON 4507 tensile machine (at a rate of 2mm/min). In particular, 10 hardness and 10 electrical conductivity measures have been carried out for each heat treatment time. The values reported in the graphs are the average ± the standard deviation.
Samples for microstructural investigations have been prepared by traditional methods and observed by a NIKON EPIPHOT 200 light microscope and by a PHILIPS XL 40 scanning electron microscope equipped with EDS. The regions considered for damage evaluation extends along the tensile axis of the samples, from the fracture surface to the head of the specimen where no broken particles are detected, at a distance of 2.5-5 mm one from each other. The average size and the number of damaged particles have been revealed manually by using the Lucia v. 4.51 software for image analysis. A 1000x magnification has been used in the light microscope corresponding to a frame area of 139x101μm^2 .

TABLE 1: A356 ALLOY CHEMICAL COMPOSITION (WT%)

Si	Fe	Cu	Mn	Mg	Ni	Zn	Pb+Sn	Ti	Sr	Others	Al
6.5	0.15	0.03	0.03	0.30	0.03	0.05	0.03	0.20	0.01	0.10	Rem

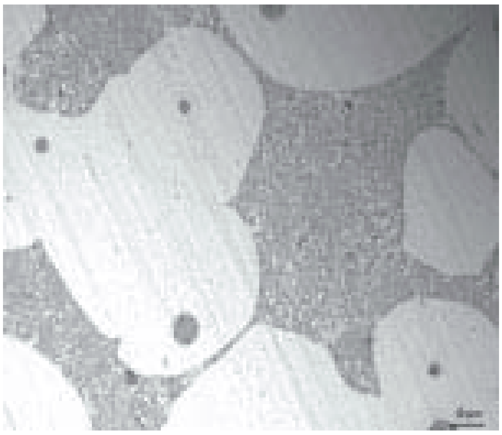

Fig. 1: Light microscopy of the as received A356.

RESULTS AND DISCUSSION

Fig. 1 shows the globules of the primary phase (alpha), resulting from the electro-magnetic stirring, bounded by the eutectic phase as appearing at the light microscope. Eutectic is also entrapped inside the globules.
The EDS analysis has revealed the chemical composition of the areas marked in Fig. 2.
The globules (area 1) are mainly Al with Mg in very low quantities, while the lighter phase in the eutectic region (area 2) are rich in Mg and Fe. Fe is combined with other elements to form irregular particles of AlFeSi or lamellar particles of $Fe_2Si_2Al_9$ or $FeAl_3$. Magnesium is instead present in the Mg_2Si or with aluminium in the form of Mg_2Al_3 (5,6). The darker area of the eutectic, (area 3), is rich of Si particles and in minor parts of Mg_2Si (5,6).
Fig. 3 shows a BSE image of sample solution treated at 540°C for 1 hr. The exposure at high temperature has induced the spheroidisation of silicon,

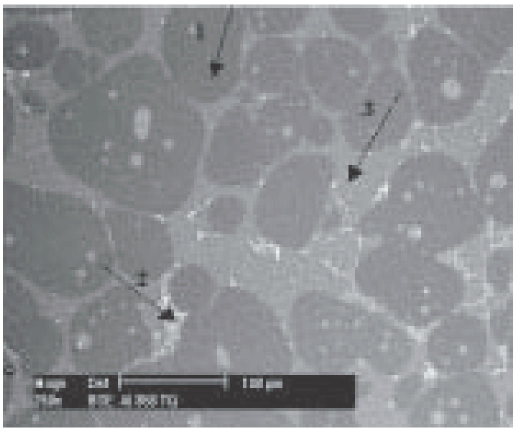

Fig. 2: SEM image of as-received sample.

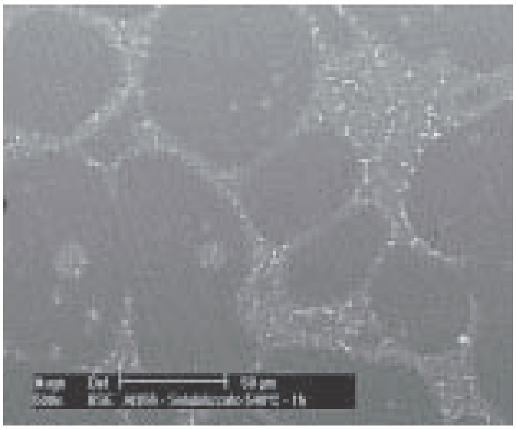

Fig. 3: Fig. 3: SEM image of the sample exposed at 540°C for 1 hour.

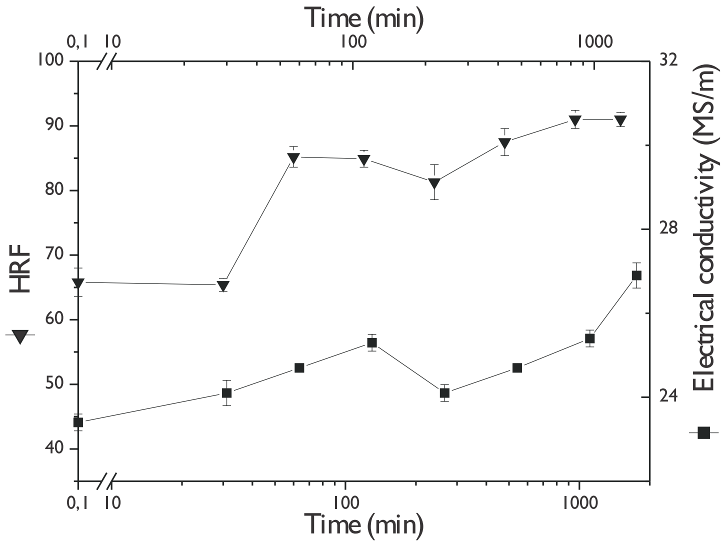

Fig. 4: Ageing curve and electrical conductivity measurements at 160°C .

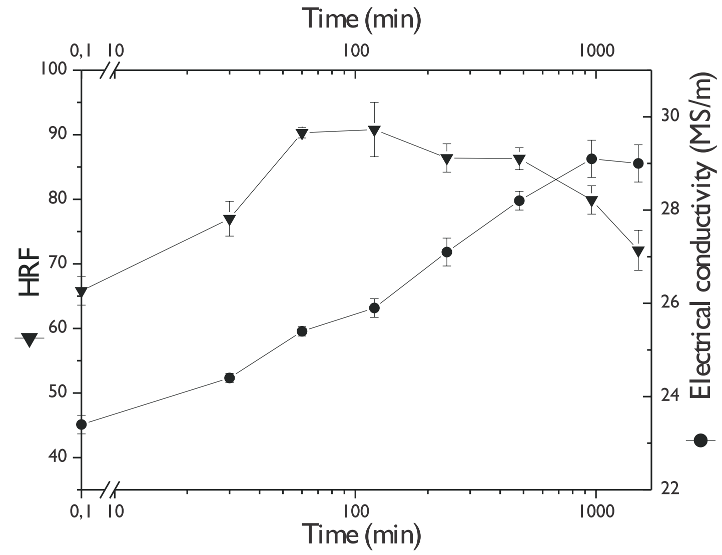

Fig. 5: Ageing curve and electrical conductivity measurements at 200°C.

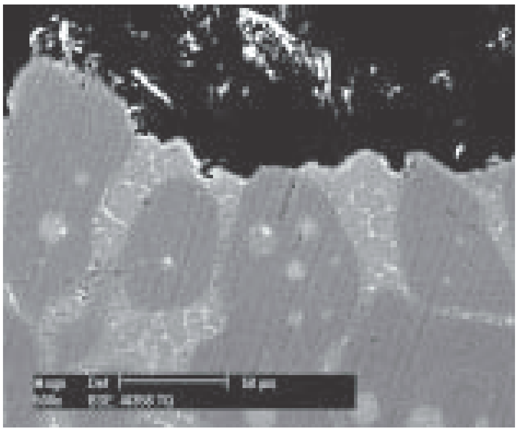

Fig. 5: Ageing curve and electrical conductivity measurements at 200°C.

due to solid state diffusion phenomena. Moreover, EDS analysis has detected a reduction of magnesium content in the eutectic region and the disappearance of the Mg_2Si compound.

Figures 4 and show the hardness and electrical conductivity values of specimens aged at 160°C and 200°C.

The ageing behaviour appears to be different at the temperatures considered. At 200°C the overageing occurs after 2 h., while at 160°C it is not revealed in the time considered. Instead, the electrical conductivity increases with time at both temperatures, thus indicating that atoms in solid solution can still contribute to precipitation.

Table 2 reports tensile values of heat treated samples. The values allow to assess that the microstructural changes like silicon spheroidisation induced by solution treatment, increase ductility without decreasing tensile strength if compared to the as received material where silicon has a lamellar shape. The elongation to fracture substantially increases at low aging times respect to the as-thixo condition with no modifications in tensile strength.

Table 2. Tensile properties of the A356 thixocast alloy after different heat treatments.

Heat treatment	Yield Strength (MPa)	UTS, (MPa)	Elong. to fracture, (%)	Young's Modulus, (GPa)
As-thixo	104	241	12	78
540°C, 1h	106	231	18	92
+ 160°C, 0.5h	115	244	20	79
+ 160°C, 4h	127	245	18	90
+ 160°C, 25h	153	264	16	86
+ 200°C, 0.5h	111	236	16	91
+ 200°C, 2h	154	257	15	89

SEM analysis of polished longitudinal sections has evidenced that fracture propagates in the eutectic region around the globules, in each heat-treated sample (Fig. 6). This probably arises from microvoids nucleating (around) in Si particles, and, when the tensile stress increases, their coalescence leads to sample breaking (1).

Fig. 7 reports the fracture surface of the as-thixo sample. The presence of cleavage planes and the intergranular shape indicate a brittle behaviour due to the lamellar microstructure of Si particles in the eutectic.
Fig. 8 shows the dimples left by broken silicon particles after plastic deformation of the matrix in the solution treated sample. The solution treated and aged sample too exhibit a ductile behaviour of the fracture surface, because of Si spheroidisation during exposure at 540°C for 1h. The microstructure analysis carried out on solubilised and aged samples has confirmed that particle dimension (3) is not the fundamental factor for inducing the fracture process, while it is important to remark that the aspect ratio controls particle fracture, i.e. elongated particles break more frequently than the spherical ones (4).
Moreover, a silicon particle may fracture in several points but always perpendicularly to the tensile direction. In few cases, silicon particle decohesion from the matrix has also been observed. All these features implicate that Si particle breaking greatly depends from local conditions which may include particle orientation, activation of slip planes and dislocation accumulation mechanism (3).
Figures 9 and 10 report the silicon particles damage frequency as a function of the relative distance from the fracture surface (mm/mm) for samples solubilised at 540°C for 1 h and aged at 160°C and 200°. The frequency of damaged silicon particles is high in proximity of the fracture surface confirming that their fracture is the main cause for the decreasing of mechanical properties of the alloy (3) and that the damage increases with plastic deformation. In particular, the maximum damage value decreases when ageing time increases.
The result confirms the theory (3) by which silicon particle damage occurs due to dislocation accumulation mechanisms. Infact the hardness influences the ability of ametal to be plastically deformed and harder the alloy is, more obstacles to dislocation mobility (such as GP zones and coherent or semi-coherent precipitates) are present. Consequently, the interaction of dislocations with silicon particles will be less probable and the frequency of broken particles decreases. Plastic deformation and thus the elongation to fracture will be a consequence of the constraint to dislocation movements given by precipitation hardening, as it is confirmed by tensile test results in Table 2.

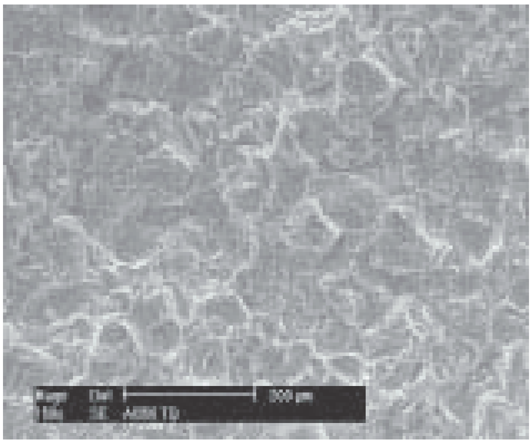

Fig. 7: Fracture surface in the as-thixo sample.

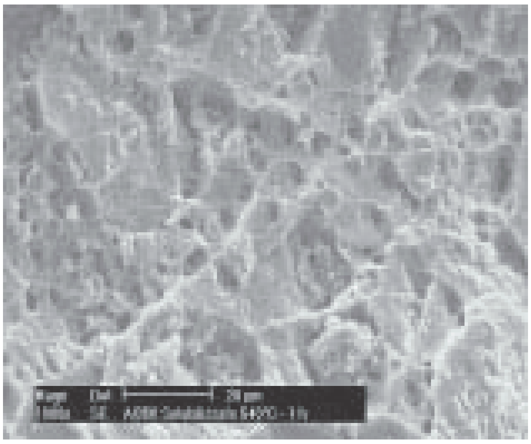

Fig. 7: Fracture surface in the as-thixo sample.

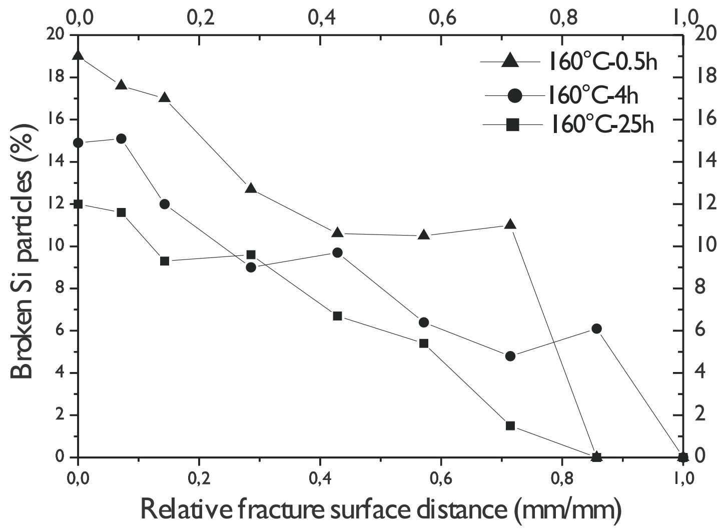

Fig. 4: Ageing curve and electrical conductivity measurements at 160°C .

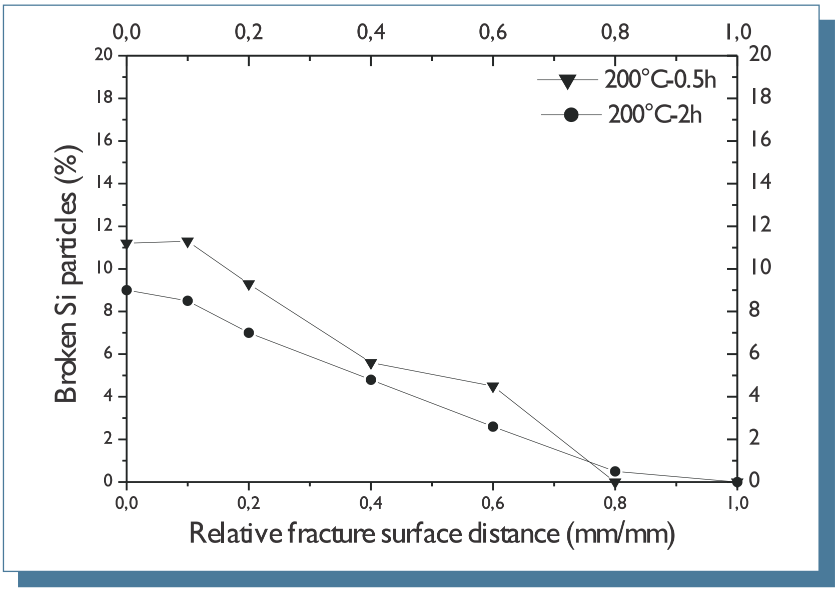

Fig. 10: Fraction of broken Si particles vs relative fracture distance at 200°C.

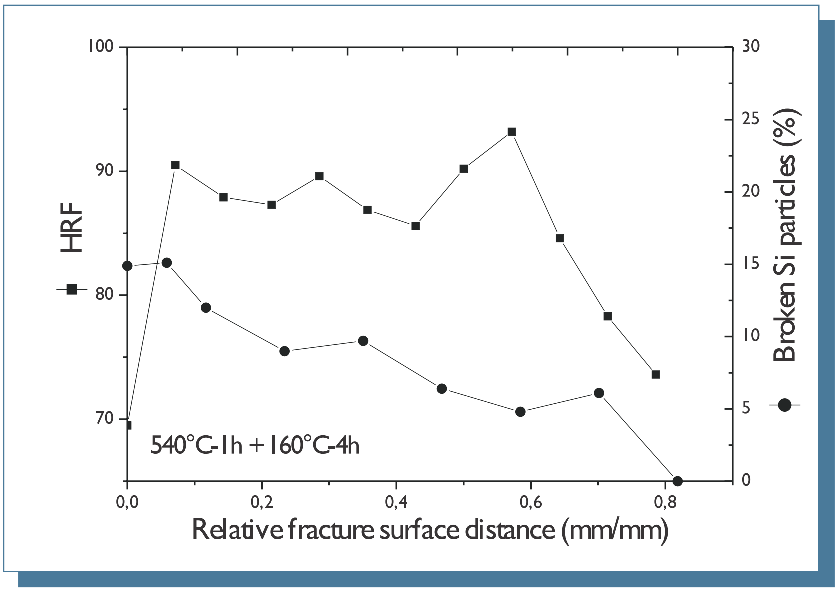

Fig. 11: Comparison between hardness curve and fraction of broken particles curve for specimen aged 4hours at 160°C.

The hardness profile is measured along the main axis, from the fracture surface to the shoulder of the sample. The trend is the same for all treatment conditions starting at the fracture surface, increasing to a plateau in the gauge length and then decreasing in proximity of the head-junction as shown in Fig. 11. Moreover, in the same graph, the damage is illustrated to demonstrate that, even if it decreases with distance, it is not the factor which greatly influences the hardness of the alloy after tensile test as it would have been if the hardness and damage curves had opposite trend.

CONCLUSION

The study of A356 thixocast alloy damage has led to the following conclusions:

1. The dimension of the particles is not a fundamental factor in determining sample fracture, while the shape, i.e. the aspect ratio, is important since it has been observed that elongated particles break more frequently than the spherical ones (3,4).
2. The percentage of broken silicon particles decreases with increasing hardness (precipitation hardening).
3. The percentage of broken silicon particles increases with sample straining.
4. Particles fracture because of stress concentration given by dislocation accumulation.

REFERENCES

[1] C. H. Caceres, C. J. Davidson, J. Grifiths: The deformation and fracture behaviour of an Al-Si-Mg casting alloy", Material Science and Engineering A197 (1995), 171-179.

[2] C. H. Caceres, B. I. Selling: Casting defects and tensile properties of an Al-Si-Mg casting alloy", Material Science and Engineering A220 (1996), 109-116

[3] J. W. Yeh, W.P. Liu: The cracking mechanism of silicon particles in an A357 aluminum alloy", Metallurgical and Material Transactions, 27A, (1996), 3558-3568.

[4] A. M. Gorkhale, M. D. Dighe, M. Horstmeyer,: "Effect of temperature on silicon particle damage in A356 alloy", Metallurgical and Material Transactions, 29A, 1(998), 905-907.

[5] ASM Hand Book "Aluminum alloy", Vol 9, pag. 351-388

[6] POLMEAR: "Light Alloys, Metallurgy of Light Metals", Arnold Publ.